Materials Physics and Mechanics. 2023;51(1): 61-67
Research article
http://dx.doi.org/10.18149/MPM.5112023_6

Submitted: August 8, 2022
Approved: November 7, 2022
Accepted: November 18, 2022

Simulation of the plastic deformation of shape memory alloys considering shear anisotropy on the slip plane

F.S. Belyaev [1] ✉, M.E. Evard [2], A.E. Volkov [2]

[1]Institute for Problems of Mechanical Engineering RAS, 61, Bolshoi Pr. V.O., St. Petersburg, Russia, 199178

[2]St. Petersburg State University, Universitetskaya emb., 7-9, St. Petersburg, Russia, 199034

✉ belyaev_fs@mail.ru

Abstract. The plastic deformation of a TiNi single crystal was modeled, taking into account the anisotropy of the yield stress in the slip plane. The material parameters (initial yield stress and hardening factor) were selected for each slip system. Deformation curves were obtained for different orientations of the single crystal. It is shown that Schmid's law prevents obtaining a correct description of deformation for all orientations of single crystals. Good agreement with experiments was observed for the crystal orientations ⟨001⟩, ⟨111⟩, and ⟨123⟩ but not ⟨011⟩, for which the deformation mechanism was different. In the case of the deformation of a polycrystalline sample, the anisotropy in the slip plane is not significant.
Keywords: shape memory alloys, microstructural modeling, plastic deformation, TiNi, single crystal, polycrystal

Acknowledgments. *This research was funded by Russian Foundation for Basic Research (RFBR), project number 19-31-60035.*

Citation: Belyaev FS, Evard ME, Volkov AE. Simulation of the plastic deformation of shape memory alloys considering shear anisotropy on the slip plane. *Materials Physics and Mechanics*. 2023;51(1): 61-67. DOI: 10.18149/MPM.5112023_6.

Introduction

Shape memory alloys (SMA) are intelligent materials that can exhibit functional properties such as shape memory and superelasticity. Due to their unique properties, these alloys are widely applied in the fields of aerospace, biomedical and micro-electromechanical systems (MEMS) and so on [1-4]. Plastic deformation is an important phenomenon associated with the thermomechanical properties of SMA. This association is because the dislocation slip in these materials is not only one of the deformation mechanisms but also leads to the formation of several specific effects, such as two-way shape memory and the “training” of the material. Plastic deformation under certain conditions makes it possible to purposefully improve the properties of materials. The influence of plastic deformation on the mechanical behavior of SMA is of considerable interest to researchers [5-9].

Successful development of devices with SMA parts requires a reliable method for calculating their mechanical behavior. Most of the existing models of SMA aim to describe phase transformations since phase deformations and the realization of functional properties are associated with them. However, some models also describe plastic deformation. Phenomenological models describing plastic deformation include [10-12]. In the one-dimensional model of Tanaka et al. [10], plastic deformation is associated with residual stresses under cyclic loading. In the model used by Bo et al. [11], thermally induced

transformation and its interaction with plastic deformation under cyclic loading conditions are considered. The model in [12] describes stress-induced phase transformations and plastic strain. In this model, the development of the plastic strain is associated with detwinned martensite and is induced by cyclic loading conditions. The earliest microstructural models describing plastic strain are [13-15]. These models describe only microplastic deformation, that is, plastic deformation associated with the accommodation of growing martensite plates. In [13], it is assumed that microplastic deformation increases with the motion of the interphase boundaries. In [14-15], microplastic flow conditions similar to the flow conditions in the one-dimensional case with isotropic hardening are proposed. The models in [16-17] describe active plastic deformation, that is, plastic deformation associated with dislocation slip. The model in [16] describes the martensite plasticity present only after the austenite–martensite transformation is complete. The model in work [17] accounts for both phase transformations and plasticity at the crystallographic level and allows their simultaneous realization. The most recent works on the microstructural modeling of SMA that consider plastic deformation include [18-27]. In works [18-21] a microstructural model is presented that describes the plastic deformation of austenite and martensite, as well as the accumulation of plastic deformation under cyclic loading. The models of [22-25] describe dislocation slip in austenite but not the deformation twinning of martensite. The model of Xu et al. [26] describes the austenitic plasticity caused by dislocation slipping, and the martensitic plasticity caused by dislocation slipping and deformation twinning. It also describes the effect of grain size on martensitic transformations. The model of Ju et al. [27] describes the SMA deformation in terms of finite deformations. It takes into account both microplastic deformation and plastic deformation of austenite and martensite.

Earlier authors developed the model to describe microplastic strain and its effect on the functional properties of SMA [28-29], but it was unable to describe active plastic strain. Based on this, the purpose of this work is to describe the active plastic deformation of the SMA as a separate deformation mechanism. Moreover, the model should be able to describe the deformation of both single crystals and polycrystalline samples. During the deformation of single crystal samples, the flow stress depends on the orientation of the tension axis. To account for this when describing SMA deformation, it is necessary to include an elementary act of plastic deformation in the model: dislocation shear and its anisotropy on the slip plane.

Model

The model material is a single crystal (one grain with an orientation of crystallographic axes ω) with several slip systems. In metals and alloys, the dislocation slip occurs only on certain crystallographic planes. On other planes, it is difficult for shearing to occur, since the corresponding flow stresses exceed the ultimate strength of the material. All active slip planes can be divided into M families of crystallographically equivalent planes. Let us denote K_m as the number of planes of the family m. Then, we propose that Reuss's hypothesis is applicable. The plastic strain of model material $\varepsilon_\omega^{p(m,k)}$ is the sum of the strains on each of the slip planes:

$$\dot{\varepsilon}_\omega^{gr\,p} = \sum_{m=1}^{M} \sum_{k=1}^{Km} \dot{\varepsilon}^{p(m,k)}, \quad (1)$$

where $\varepsilon_\omega^{p(m,k)}$ is the shear strain in the k-th plane from the m-th family.

Shear on the slip plane is assumed to occur only in the direction of the smallest Burgers vector. To formulate the flow conditions, we introduce local basis coordinate systems on the slip planes. The first axis of this local coordinate system lies in the sliding plane and is directed along the possible shear direction; the second axis lies in the same plane, and the third axis is perpendicular to it. We assume that the only components of the stress related to this local basis, which produce slip on this plane, are $\tau_{31}^{(m,k)}$ and $\tau_{32}^{(m,k)}$. If we denote the stress

applied to the single crystal by σ^{gr} then the two stress components can be found using the formulae:

$$\tau_{31}^{(m,k)} = A_{p3}^{(m,k)} A_{q1}^{(m,k)} \sigma_{pq}^{gr},$$
$$\tau_{32}^{(m,k)} = A_{p3}^{(m,k)} A_{q2}^{(m,k)} \sigma_{pq}^{gr}, \quad (2)$$

where $A^{(m,k)}$ is the rotation matrix that transforms the crystallographic basis ω into the local basis of the k-th slip plane of the m-th family.

The condition for the onset of plastic shear was formulated based on Schmid's law: plastic flow begins when the shear component of the stress, $\tau_{31}{}^{(m,k)}$ or $\tau_{32}{}^{(m,k)}$, reaches a critical value, $\tau^{s(m,k)}$, for the given slip system:

$$\tau^{s\,(m,k)} = \begin{cases} \tau_{31}^{(m,k)}, if\ \tau_{31}^{(m,k)} \geq \tau_{32}^{(m,k)}, \\ \tau_{32}^{(m,k)}, if\ \tau_{31}^{(m,k)} < \tau_{32}^{(m,k)}. \end{cases} \quad (3)$$

We assume that the flow stress $\tau^{s(m,k)}$ is the sum of the initial (equilibrium) value $\tau^{s(m,k)}{}_{eq}$ and the deformation additive $\tau^{s(m,k)}{}_{def}$ is responsible for the strain hardening:

$$\tau^{s(m,k)} = \tau_{eq}^{s(m,k)} + \tau_{def}^{s(m,k)}. \quad (4)$$

The value of the initial flow stress $\tau^{s(m,k)}{}_{eq}$ is the same for all planes belonging to the given m-th family. To calculate the value of $\tau^{s(m,k)}{}_{def}$, we assume that the hardening factor h^m does not depend on the shear value and the strain rate. It is equal to the product of the hardening factor h^m and the maximum plastic shear rate, $\dot{\beta}_{31}$ or $\dot{\beta}_{32}$:

$$\dot{\tau}_{def}^{s(m,k)} = \begin{cases} h^m \left|\dot{\beta}_{31}^{(m,k)}\right|, if\ \left|\dot{\beta}_{31}^{(m,k)}\right| > 0, \\ h^m \left|\dot{\beta}_{32}^{(m,k)}\right|, if\ \left|\dot{\beta}_{32}^{(m,k)}\right| > 0. \end{cases} \quad (5)$$

The solution of the system of equations (2)-(5) makes it possible to calculate the $\varepsilon^{p\,(m,k)}$ components. Then the sum (1) will give the total plastic deformation of the model single crystal. To solve the system of differential equations, a direct finite-difference scheme was used.

Simulation results

To test the model, numerical experiments were conducted by stretching single crystals of TiNi alloy with different crystal lattice orientations. This alloy is very popular and widely used. It is known that plastic shear in the austenitic B2 phase of TiNi SMA slip occurs on the planes belonging to two families: {110} and {100}. The first family consists of 6 planes, and the second consists of 3 planes [30]. For the TiNi slip systems, the following material constants were selected: the initial flow stress $\tau^{s}{}_{eq}$ and the hardening coefficient h (Table 1).

Table 1. Flow stress and hardening factor for existing slip systems

Slip plane family	Initial flow stress $\tau^{s}{}_{eq}$, MPa	Hardening coefficient h, MPa
{100}	85	100
{110}	100	3000

All calculations were performed at 600 K, which is much higher than the final temperature of the reverse martensitic transformation. The choice of temperature is because an increase in stress does not cause a martensitic transformation, and plastic shear remains the only active mechanism of inelastic deformation. Figure 1 shows the results of modeling the behavior of a TiNi single crystal under tension along the ⟨001⟩, ⟨111⟩, ⟨123⟩, and ⟨011⟩ directions and the corresponding experimental dependences [30].

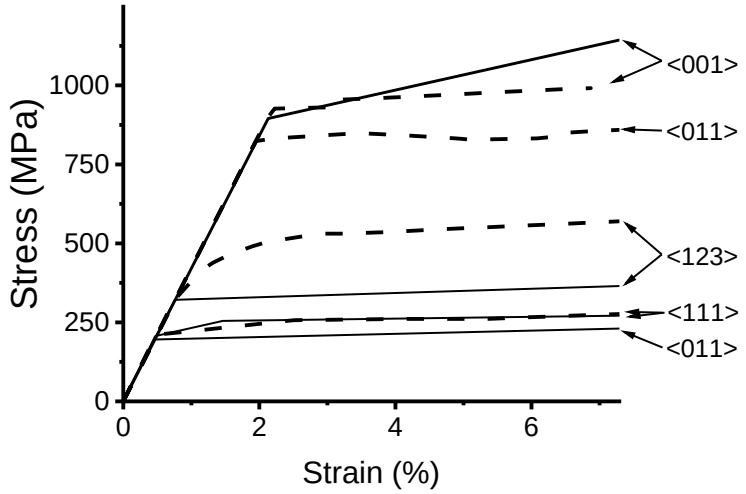

Fig. 1. Experimental [30] (dashed lines) and calculated (solid lines) tension curves of a TiNi single crystal

Comparing the calculated tension curves of a TiNi single crystal with the experimental data (Fig. 1) shows that the selected values of the material constants correctly describe the model alloy behavior with the tension oriented along the ⟨001⟩ and ⟨111⟩ axes. For the ⟨123⟩ direction, the calculated yield stress coincides with that observed experimentally [30]. For the orientation of the tension along the ⟨011⟩ direction, the calculated curve does not substantially coincide with the experimental one.

Experimental data show that under tension applied along the ⟨011⟩ direction, the crystals are "hard", that is, they have a high yield point, $\sigma_{0.1} \approx 920$ MPa [30]. In works [30-31], it was suggested that when the orientation of the tension axis changes to directions near ⟨011⟩, the deformation mechanism changes at the microscale. In particular, with the orientation ⟨011⟩, volumetric splitting of the screw dislocation core occurs, which obstructs the onset of plastic shear. Therefore, within the framework of this model, considering only the anisotropy in the slip plane does not allow an adequate description of the behavior of a TiNi single crystal for all directions of tension.

Deformation of polycrystals

The proposed model can be adapted to the calculation of the plastic deformation of a polycrystalline sample. We assume that the described representative volume consists of grains of equal size with different orientations of the crystallographic axes: 1, 2,..., ω,..., Ω. Then we can calculate the deformations of individual grains according to the proposed model and obtain the deformation of the representative volume through orientational averaging:

$$\varepsilon^p = \frac{1}{\Omega}\sum_{\omega=1}^{\Omega} R_\omega \varepsilon_\omega^{gr\,p} R_\omega^{-1}, \qquad (6)$$

where R_ω is the rotation matrix that transforms the laboratory basis to the crystallographic basis of the grain ω.

Figure 2 shows the tension curve of the polycrystal calculated by our model (solid line). The relatively low yield stress of the TiNi polycrystal is due to the action of a large number of slip systems; deformation occurs along those with lower microscopic yield stress.

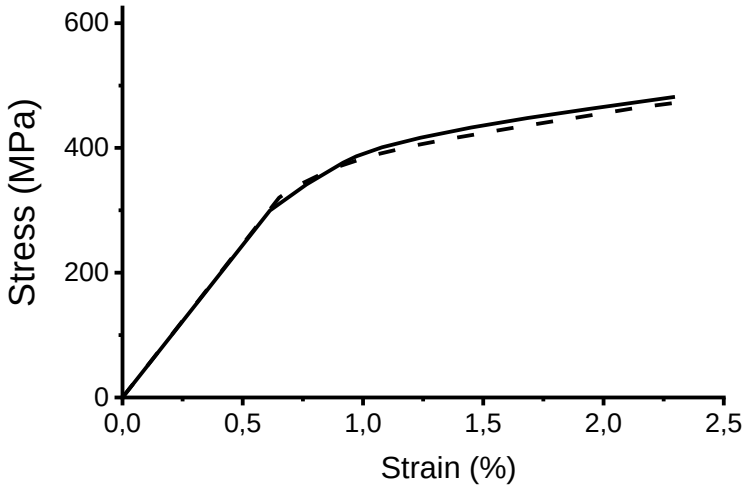

Fig. 2. Tension curves of a TiNi polycrystal calculated by a model with anisotropic (solid line) and isotropic (dashed line) shear on the slip plane

To calculate the deformation of the polycrystal, a simplified version of the model can be used that does not account for the shear anisotropy on the slip plane. A condition similar to the von Mises yield criterion but for the two-dimensional case is used for the determination of the initiation of plastic flow:

$$T_\tau = \sqrt{(\tau_{31})^2 + (\tau_{32})^2} = \tau^s. \quad (7)$$

The hardening law also changes:

$$\dot{\tau}^s_{def} = h\sqrt{\left(\dot{\beta}_{31}\right)^2 + \left(\dot{\beta}_{32}\right)^2}. \quad (8)$$

This version of the model assumes that the shear on the slip plane can occur isotropically and not only in the direction of the smallest Burgers vector. This model can describe the polycrystal behavior well, but it is not suitable for calculating the deformation of a single crystal, in which shear can occur only in certain crystallographic directions.

The calculated tension curve of a polycrystalline sample obtained by the model with isotropic shear is shown in Fig. 2 (dashed line). The results of modeling the deformation of the polycrystalline sample obtained by both models almost coincide. Accounting for anisotropy does not play an important role in modeling the polycrystal deformation because the difference in shear directions in these models ceases to significantly affect the material behavior after averaging over all grains.

Conclusions

A model of the plastic deformation of a TiNi single crystal is formulated, which accounts for dislocation shear on slip planes occurring only in the direction of the smallest Burgers vector. The material parameters were selected: yield strength and hardening factor for TiNi slip systems. The deformation curves are calculated for different directions of the tensile axis. Comparison with the experimental data showed that the model correctly describes the deformation of TiNi single crystals for different orientations of the tension axis, except for directions close to ⟨011⟩. This exception is due to the failure of the applied condition of the onset of plastic shear to account for possible changes in the deformation mechanism, particularly the splitting of the dislocation core.

A comparison of the results of the calculation according to the proposed model and according to the model allowing isotropic shear in the slip plane showed that, in the case of a polycrystalline sample, the inclusion of the anisotropy in the slip plane is not significant.

References

1. Mohd JJ, Leary M, Subic A, Gibson MA. A review of shape memory alloy research, applications and opportunities. *Mater. Des*. 2014;56: 1078-1113.
2. Choudhary N, Kaur D. Shape memory alloy thin films and heterostructures for MEMS applications: a review. *Sen. Act. A: Phys.* 2016;242: 162-181.
3. Velmurugan C, Senthilkumar V, Dinesh S, Arulkirubakaran D. Machining of NiTi-shape memory alloys - A review. *Mach. Sci. Tech.* 2018;22(3): 355-401.
4. Patel SK, Behera B, Swain B, Roshan R, Sahoo D, Behera A. A review on NiTi alloys for biomedical applications and their biocompatibility. *Mater. Today: Proc.* 2020;33: 5548-5551.
5. Levitas VI, Javanbakht M. Interaction of phase transformations and plasticity at the nanoscale: phase field approach. *Mater. Today: Proc.* 2015;2: S493-S498.
6. Prokoshkin SD. Regulation of the functional properties of shape memory alloys using thermomechanical treatment. In: Trochu F, Brailovski V, Galibois A (eds.) *Shape Memory Alloys: Fundamentals, Modeling and Industrial Applications, Proceedings of COM 1999, Canadian Institute of Mining, Metallurgy and Petroleum.* Montreal: Canada; 1999. p.267-277.
7. Shoichi E. Two-way shape memory effect generated by deformation of parent phase in Ni-Ti. In: *Proceedings of ICOMAT 1992, Monterey Institute for Advanced Studies*. Monterey, California: USA; 1993. p.965-970.
8. Zel'dovich VI, Sobyanina GA, Rinkevich OS. Influence of prestrain on the shape-memory effect and martensite structure in titanium nickelide: I. Dilatometric effects of martensitic transformations. *Phys. Met. Metallogr.* 1996;81: 305-312.
9. Belyaev SP, Resnina NN, Volkov AE. Influence of irreversible plastic deformation on the martensitic transformation and shape memory effect in TiNi alloy. *Mater. Sci. Eng.: A.* 2006;438-440: 627-629.
10. Tanaka K, Nishimura F, Hayashi T, Tobushi H, Lexcellent C. Phenomenological analysis on subloops and cyclic behavior in shape memory alloys under mechanical and/or thermal loads. *Mech. Mater.* 1995;19: 281-292.
11. Bo Z, Lagoudas DC. Thermomechanical modeling of polycrystalline SMAs under cyclic loading. Part I. Theoretical derivations. *Int. J. Eng. Sci.* 1999;37(9): 1089-1140.
12. Lagoudas DC, Entchev PB. Modeling of transformation-induced plasticity and its effect on the behavior of porous shape memory alloys. Part I. Constitutive model for fully dense SMAs. *Mech. Mater.* 2004;36(9): 865-892.
13. Sun Q-P, Lexcellent C. On the unified micromechanics constitutive description of one-way and two-way shape memory effects. *J. Phys. IV.* 1996;06(C1): 367-375.
14. Evard ME, Volkov AE. Modeling of martensite accommodation effect on mechanical behavior of shape memory alloys. *J. Eng. Mater. Technol.* 1999;121(1): 102-104.
15. Volkov AE, Casciati F. Simulation of dislocation and transformation plasticity in shape memory alloy polycrystals. In: Auricchio F, Faravelli L, Magonette G, Torra V. (eds.) *Shape memory alloys. Advances in modelling and applications, Proceedings of CIMNE*. Barcelona: Spain; 2001. p.88-104.
16. Wang XM, Xu BX, Yue ZF. Micromechanical modelling of the effect of plastic deformation on the mechanical behaviour in pseudoelastic shape memory alloys. *Int. J. Plast.* 2008;24(8): 1307-1332.
17. Manchiraju S, Anderson PM. Coupling between martensitic phase transformations and plasticity: a microstructure-based finite element model. *Int. J. Plast.* 2010;26(10): 1508-1526.
18. Yu C, Kang G, Song D, Kan Q. Micromechanical constitutive model considering plasticity for super-elastic NiTi shape memory alloy. *Computational Mater. Sci.* 2012;56: 1-5.

19. Yu C, Kang G, Kan Q, Song D. A micromechanical constitutive model based on crystal plasticity for thermo-mechanical cyclic deformation of NiTi shape memory alloys. *Int. J. Plasticity.* 2013;44: 161-191.
20. Yu C, Kang G, Kan Q. Crystal plasticity based constitutive model of NiTi shape memory alloy considering different mechanisms of inelastic deformation. *Int. J. Plasticity.* 2014;54: 132-162.
21. Yu C, Kang G, Song D, Kan Q. Effect of martensite reorientation and reorientation-induced plasticity on multiaxial transformation ratchetting of super-elastic NiTi shape memory alloy: New consideration in constitutive model. *Int. J. Plasticity.* 2015;67: 69-101.
22. Dhala S, Mishra S, Tewari A, Alankar A. Modeling of finite deformation of pseudoelastic NiTi shape memory alloy considering various inelasticity mechanisms. *Int. J. Plast.* 2019;115: 216-237.
23. Xie X, Kang G, Kan Q, Yu C, Peng Q. Phase field modeling to transformation induced plasticity in super-elastic NiTi shape memory alloy single crystal. *Modelling Simul. Mater. Sci. Eng.* 2019;27(4): 045001.
24. Xie X, Kang G, Kan Q, Yu C. Phase-field theory based finite element simulation on thermo-mechanical cyclic deformation of polycrystalline super-elastic NiTi shape memory alloy. *Comput. Mater. Sci.* 2020;184: 109899.
25. Hossain M, Baxevanis T. A finite strain thermomechanically-coupled constitutive model for phase transformation and (transformation-induced) plastic deformation in NiTi single crystals. *Int. J. Plast.* 2021;139: 102957.
26. Xu B, Yu C, Kang G. Phase field study on the microscopic mechanism of grain size dependent cyclic degradation of super-elasticity and shape memory effect in nano-polycrystalline NiTi alloys. *Int. J. Plast.* 2021;145: 103075.
27. Ju X, Moumni Z, Zhang Y, Zhang F, Zhu J, Chen Z, Zhang W. A multi-physics, multi-scale and finite strain crystal plasticity-based model for pseudoelastic NiTi shape memory alloy. *Int. J. Plast.* 2022;148: 103146.
28. Belyaev FS, Evard ME, Volkov AE, Volkova NA. A microstructural model of SMA with microplastic deformation and defects accumulation: application to thermocyclic loading. *Mater. Today: Proc.* 2015;2(3): S583-S587.
29. Belyaev FS, Volkov AE, Evard ME. Microstructural modeling of fatigue fracture of shape memory alloys at thermomechanical cyclic loading. *AIP Conf. Proc.* 2018;1959: 070003.
30. Chumlyakov YI, Surikova NS, Korotaev AD. Orientation dependence of strength and plasticity of titanium nickelide single crystals. *Phys. Met. Metallogr.* 1996;82(1): 102-109.
31. Surikova NS, Chumlyakov YI. Mechanisms of plastic deformation of the titanium nickelide single crystals. *Phys. Met. Metallogr.* 2000;89(2): 98-107.

THE AUTHORS

Belyaev F.S.
e-mail: belyaev_fs@mail.ru

Evard M.E.
e-mail: m.evard@spbu.ru

Volkov A.E.
e-mail: a.volkov@spbu.ru